

## THE STARBURST-AGN CONNECTION: INTEGRAL FIELD SPECTROSCOPY OF MERGING AND SEYFERT 2 GALAXIES

SARAH A. JAEGLI<sup>1</sup> AND ROBERT D. JOSEPH<sup>2</sup>

Institute for Astronomy, University of Hawai'i at Manoa, Honolulu, HI 96822

*Draft version July 6, 2007*

### ABSTRACT

Infrared bright galactic nuclei may be powered by accretion of matter onto a black hole, a burst of new star formation, or both of these processes. To gain insight into such processes we have used integral field spectroscopy to observe a sample of galaxies with identified AGN or nuclear starbursts. We confirm the presence of a starburst in the nuclear regions of the galaxies IC 3639, MRK 477, NGC 2623, and NGC 3227. Using diagnostics derived from the H and K-band spectra and the stellar synthesis model Starburst 99 we determine ages for the starbursts. We find self-consistent starburst models to account for the Hydrogen recombination line emission, the [Fe II] emission from supernova remnants, and the K-band continuum luminosity. We confirm that these Seyfert 2 nuclei do indeed have associated starbursts.

*Subject headings:* galaxies: starburst — galaxies: Seyfert 2 — infrared: galaxies

### 1. INTRODUCTION

Luminous galactic nuclei can be powered by two different mechanisms. In one mechanism matter is accreted onto a super-massive black hole at the galactic nucleus. The other mechanism involves a rapid burst of star formation that produces many luminous young stars, a "starburst." Both events occur inside a large optical depth of dust: an active galactic nucleus through its dusty torus and starbursts through their dusty cocoons. Historically there has been debate regarding the identity of infrared bright galactic nuclei but a number of clear cases of nuclear star formation have been found in galaxies previously thought to only have an AGN. NGC 1068, NGC 5135, and NGC 6240 have all been thoroughly investigated and found to host composite nuclei.

A composite galactic nucleus is one which is host to an actively accreting massive black hole and a population of newly formed stars coexisting with the old nuclear population. Such objects may hold the key to understanding galactic evolution in the low redshift universe. In the unified model of an active galactic nucleus (AGN) a Seyfert 2 represents an observer's position where the energetic accretion of matter onto the central black hole is hidden by a dusty torus of surrounding material of many tens of parsec in size. The sudden onset of star formation near the galactic nucleus involves the formation of many young stars within dusty nebular cocoons. The O and B type stars which are the largest and brightest dominate the light output from the starburst and drown out the dimmer young stars and the older stellar population. Gonzalez-Delgado, Heckman, & Leitherer (2001) investigate a sample of 20 Seyfert 2 nuclei looking for traces of these young hot stars using near-ultraviolet spectral diagnostics and identify them in approximately half of their sample.

The formation of both nuclear starbursts and AGNs requires that new material is rapidly funneled into the nucleus to provide the necessary fuel. Galactic interac-

tions are the most obvious source of such material. Non-axisymmetric gravitational perturbation of a galaxy can cause a rearrangement of matter and can send gas spiraling into the core. Galaxy mergers provide both material and a mechanism for a new starburst or fueling an AGN. The presence of a nuclear starburst or an AGN is strongly correlated with the presence of companion galaxies as shown by Storchi-Bergmann et al. (2001), however interactions are not the only way to incite nuclear activity. Bars in spiral galaxies have long been thought to funnel material into the nucleus (Barnes & Hernquist 1996).

Nuclear starbursts and AGN overlap in space and, for a few cases, in time. Energy and angular momentum arguments show that it takes very little mass to produce the observable massive energy of an AGN, but it is difficult to "feed the monster" directly, as the AGN is referred to in Gunn (1977). Nuclear starbursts are able to form much more easily and as the starburst ages supernovae near the nuclei can feed an AGN with their tenuous winds. AGN may heat and compress nearby neutral medium, leading to more star formation. These last two processes provide the possibility for an interesting feedback mechanism between the starbursts and AGNs in composite nuclei. In many cases it may be necessary to have a nuclear starburst process new material and then feed it to the black hole, causing an AGN to light up.

Because of the extinction problem, using optical diagnostics for AGN and starbursts can be problematic. However, at 2 microns the obscuration due to dust is ten times less than at visible wavelengths making it possible to see through the clouds of dust to the luminous source hidden within. Using the UIST integral field unit on the United Kingdom Infrared Telescope (UKIRT) we make observations of merging and Seyfert 2 galaxies in the H and K-bands to identify these luminosity sources spectrally and look for evidence of the starburst-AGN connection.

### 2. DATA

We have selected four galaxies out of available data for about 20 similar objects. IC 3639, MRK 477, NGC 2623, and NGC 3227 were chosen for analysis because there is

<sup>1</sup> graduate student whose 699 project this represents

<sup>2</sup> 699 project advisor

relatively little published on them and they reflect the variety of objects found in the rest of the data.

### 2.1. Observations

Observations were obtained by R. Joseph on April 19, 20, 21, 22, and 23, 2003 using the integral field unit of the UKIRT Imager-Spectrometer described by Ramsay-Howat et al. (2004). The integral field unit has a  $6 \times 3.3$  arcsec<sup>2</sup> field of view and is composed of 14 image-slicing mirrors of  $6 \times 0.24$  arcsec<sup>2</sup>. The image slicer redirects the light so that the slices are vertically aligned when passing through the grism onto the array. Using the HK grism provided a resolution of 900 with a range of 1.4-2.4 microns on the detector. All of the observations presented here were taken with the slit unit at a position -90.0deg East of North. Integration times for all observations were 288 seconds.

### 2.2. Data Reduction

The data was reduced with the Starlink data pipeline specific to the IFU. The pipeline has applied darks and flats to the data. A linear solution to the dispersion of wavelength on the detector has been determined from arc lamp spectra. Corrections for the loss of spectral energy due to the instrument and detector were determined using calibration fields from a lamp with a known SED. Flux calibrations were applied using standard star measurements taken throughout each of the five nights. Bad pixels were removed and atmospheric absorption was subtracted. Spectra which were aligned vertically on the detector array were reordered and stacked into a data cube to correctly represent the positioning within the integral field. The end product of the pipeline is a flux calibrated data cube of dimensions  $14 \times 54 \times 1024$ . The spatial dimensions of the integral field have been reconstructed in the first two dimensions of the data cube and the third dimension contains the wavelength information. The spatial pixels of the datacube are rectangular pixels having the dimensions  $0.1199 \times 0.24$  arcsec<sup>2</sup>.

### 2.3. Additional Processing

A continuum image of each of the galaxies has been constructed by taking the sum of the flux along the wavelength dimension. These images, shown as contours, are plotted in Figure 1. The nuclei of all four galaxies show a roughly circular structure, so to increase the signal-to-noise the spectra were averaged over a circular aperture containing most of the flux from the galactic nucleus. The H and K-band portions of these spectra are shown in Figures 2-6. The wavelength scaling of the data cube spectra have been corrected for the galaxy redshift velocity,  $cz$ , listed in Table 1. Because we have used an integral field we can be sure that these spectra are a true measure of the nuclear region and no light has been missed which might be the case with long slit spectroscopy.

To facilitate analysis involving emission features in the galaxies a continuum subtracted data cube for each galaxy was constructed by smoothing each spectrum in a data cube until the sharp spectral features were gone, leaving the approximation to the continuum. This smooth continuum was subtracted from the original spectrum to get the line spectrum.

We have determined the extinction due to local galactic dust to be a negligible effect. The extinction is of the

order of a few percent, smaller than the uncertainty in the measurement of the flux.

## 3. RESULTS

### 3.1. Spectral Diagnostics

Various diagnostics can be used to determine the presence and strength of a starburst or Seyfert 2 in a galactic nucleus.

Diagnostics for starbursts are dependent on the life-cycle of the very brightest stars. The recombination lines of Hydrogen, Paschen  $\alpha$  at  $1.8756 \mu\text{m}$  and Brackett  $\gamma$  at  $2.1661 \mu\text{m}$ , are produced by massive, bright stars during their evolution on the main sequence (Bendo & Joseph 2004). For these low redshift galaxies Paschen  $\alpha$  falls in the area of atmospheric absorption between the H and K bands. Although it is exceedingly bright Paschen  $\alpha$  cannot be used quantitatively due to uncertainty of the atmospheric correction. He I at  $2.0587 \mu\text{m}$  is produced by young massive O-type main sequence stars with formidable winds (Kudritzki 1998). As the brightest stellar members of a starburst die the powerful continuum of these stars is lost but large amounts of energy are released into the surrounding environment. Emission in galaxies from [Fe II] at  $1.6440 \mu\text{m}$  is produced almost entirely in supernova remnants or their outflows and lasts for  $\sim 10^4$  years after the supernova (Alonso-Herrero et al. 2003).

In slightly older starbursts the early spectral types of stars have vanished and later spectral types dominate the continuum emission. The absorption of the Si I at  $1.5890 \mu\text{m}$  and the CO (6-3) band at  $1.6189 \mu\text{m}$  in the atmospheres of G, K and M-type red giants can be used to characterize the H-band spectrum of older starbursts (Origilia, Moorwood, & Oliva 1993). The CO (2-0) band beginning at  $2.2935 \mu\text{m}$  in the K-band is produced by the same stellar population as the Si I line and CO (6-3) band head but caution must be used when applying it to the spectrum of a composite nucleus. The CO (2-0) band may be diluted by up to 80% by the underlying continuum, especially if there is an AGN present (Oliva et al. 1999).

The forbidden line of [Si VI] at  $1.9634 \mu\text{m}$  can only be produced in the region near an AGN because of the high ionization potential of Si VI (205 eV). Paschen  $\alpha$  and Brackett  $\gamma$  are also produced by AGN. These lines are produced by both broad and narrow line regions and can contaminate the relatively narrow recombination lines produced by a starburst. Strong AGN can also be identified by the strong non-thermal power law of the continuum which rises to the infrared and is the hallmark of QSOs.

H<sub>2</sub> appears in emission at several wavelengths and indicates where interstellar gas is being shocked. This emission may be the result of many processes. Shocks in neutral Hydrogen clouds can develop during the violent kinematics of a galaxy merger (van der Werf et al. 1993), which is possibly the very earliest stage of a starburst. Neutral gas can also be excited in the expanding shock wave produced when massive stars end their lives as supernovae. Finally neutral gas can become shocked by the energetics resulting from an AGN.

A summary of all of these spectral diagnostics is shown in Table 2. A summary of the relative strengths of these indicators for each of the galaxies is shown in Table 3.

### 3.2. IC 3639

IC 3639 is a barred spiral with two other companion spiral galaxies. The Seyfert 2 nucleus has been studied at X-ray wavelengths with CHANDRA (Ghosh et al. 2007), and has been found to have a discrete hard x-ray source with an extended soft x-ray halo whose size corresponds very well with the distribution of intensity that we observe shown in the first panel of Figure 1. Bransford & Appleton et al. (1998) investigated the nucleus at radio wavelengths and found a vigorous nuclear starburst which is a dominant part of the nucleus. HST imaging and spectroscopy at ultraviolet wavelengths presented by Gonzalez-Delgado et al. (1998) shows that either the starburst or the AGN is producing outflows from the nucleus. They estimate the age of the starburst at 3-5 Myr based on comparison with stellar synthesis models.

The H-band spectrum of the nuclear region of IC 3639 shows very strong [Fe II] emission. The CO 6-3 band head is visible but weak and the Si I absorption line seems lost in a neighboring absorption feature. The K-band of this galaxy is full of strong H<sub>2</sub> emission and has astoundingly strong Brackett  $\gamma$  emission. [Si VI] from the Seyfert 2 stands on the lip of an atmospheric absorption feature. He I emission is clearly visible and the feature between H<sub>2</sub> 1-0 S(1) and Brackett  $\gamma$  appears to be Mg II. The CO 2-0 band head stands out strongly, although the rest of the band seems weaker and is possibly getting diluted by continuum flux from the AGN. From the emission lines we can tell that IC 3639 has a starburst population which is still very young but which has begun to contribute a considerable amount to the [Fe II] flux through supernovae.

### 3.3. MRK 477

Markarian 477 is a compact amorphous galaxy with with a very bright Seyfert 2 nucleus which is interacting tidally with a companion galaxy. Observations of polarized optical light show that this nucleus is an obscured Seyfert 1. A low amount of obscuration due to dust in this nucleus make UV observations of this galaxy possible and Heckman et al. (1997), with their HST observations in the UV, uncover a very compact region of recent star formation. They estimate of 6 Myr based on stellar synthesis models but note that the models they use are for instantaneous formation of metal rich stars.

The H-band spectrum of MRK 477 is mostly featureless except for a massive amount of flux from the [Fe II] emission line. The continua of both H and K bands show the slight rising power law of non-thermal flux from the obscured Seyfert 1 at the core of this galaxy. [Si VI] is the strongest emission line in the K-band, but Brackett  $\gamma$  and an asymmetric H<sub>2</sub> 1-0 S(1) line are quite strong. He I is visible above a noisy continuum. The CO (2-0) absorption band is lost to noise and atmospheric features at the red end of the K-band and is diluted by the continuum flux from the Seyfert 2. The strong AGN features make MRK 477 an unexpected site for a starburst but the signature of many supernovae and hydrogen recombination together make the presence of a starburst very clear.

### 3.4. NGC 2623

NGC 2623 is a gas-rich merger of two spiral galaxies. It exhibits a knotted, complex bulge and two tidal tails, one

curling north-east to south-east and the other slanting south-west to west. Lipari et al. (2004) measure a large cone of galactic outflow of  $\sim 400 \text{ km s}^{-1}$  fanning out from the nucleus and speculate that it may be the result of the merger processes or caused by the central starburst.

The H-band of NGC 2623 is rich in absorption, however the Si I and CO (6-3) are difficult to pick out. [Fe II] provides relatively little emission in this galaxy. The K-band shows something which appears to be the [Si VI] line but is in fact an atmospheric emission line at an unfortunate wavelength. H<sub>2</sub> and He I lines are present but not strong. Brackett  $\gamma$  and the CO (2-0) band are quite strong. This galaxy is a bit of an enigma, with a strong signature of bright main sequence stars and red giants, but little contribution from supernovae. This may be a sign the the starburst is slowly ending.

### 3.5. NGC 3227

NGC 3227 is a bright, close galaxy with a Seyfert 1 nucleus and is a member of a group of 13 galaxies. Using adaptive optics Davies et al. (2006) resolve a circum-nuclear ring of a few to a few tens of parsecs where a starburst with estimated age of 40 Myr has occurred.

The spectrum of NGC 3227 has very high signal-to-noise. The H-band spectrum of this galaxy's nucleus shows fairly weak absorption features and a tiny [Fe II] flux relative to the other galaxies in the sample. The K-band features appear in exquisite detail although they have very little strength relative to the continuum. The H<sub>2</sub> (1-0) S(3), S(2), and S(1) are all present and there is the slightest hint of a He I line between them. The AGN shows a correspondingly small [Si VI] line. Brackett  $\gamma$  is weak but has a mysterious neighboring line which almost rivals the H<sub>2</sub> lines in strength. NGC 3227 hosts a miniature but perfectly formed CO (2-0) band. The diminished features of this galaxy show signs of an aging stellar population with a well hidden or weakening AGN.

## 4. DISCUSSION

### 4.1. *Starburst99*

Starburst99 is stellar synthesis code that yields a set of predictions of the parameters of an evolving stellar population based on stellar atmosphere models. Initially outlined in Leitherer et al. (1999), these new models replace the previous stellar synthesis models done by Leitherer and Heckman in 1995. The original dataset from Leitherer et al. (1999) is available electronically via the internet. Users can also run their own simulations either through the website or by downloading the source code and running simulations locally. For ease of use, uniformity, and comparability we have chosen to use the original 1999 dataset.

In the original dataset the authors have chosen two limiting star formation scenarios: continuous and instantaneous star formation. In the continuous star formation case stars are formed at a constant rate normalized to  $1 M_{\odot} \text{ yr}^{-1}$ . For the instantaneous case stars are of a single age and the simulation is normalized to a population of  $10^6 M_{\odot}$ . Three cases of the initial mass function(IMF) are considered. The reference case (model A) reproduces a traditional Salpeter IMF with a power law exponent of 2.35 and a mass range of 1-100  $M_{\odot}$ . The second case (model B) considers a steeper power law slope of 3.3 with

the same mass range of 1-100  $M_{\odot}$ . The third(model C) uses the Salpeter IMF slope of 2.35 but has a significantly lower high mass cut-off of 30  $M_{\odot}$ . Stellar populations of solar metallicity ( $Z=0.020$ ) are presented in Leitherer et al. (1999) but the metallicities  $Z=0.040, 0.008, 0.004, 0.001$  are also available in the full dataset published on the webpage. In order to cover the full lifetime of the brightest stars, models are evolved through the range of ages between 1 Myr and 1 Gyr. For each age the spectral energy distribution of the whole stellar population is determined and spectral diagnostics such as luminosity, color, line width, and line flux are calculated.

Due to the infrared nature of our spectra there are only a few Starburst99 diagnostics that we can use to identify the age and strength of the nuclear star formation in our sample four galaxies. The equivalent width of Si I and CO (6-3) band head are included as diagnostics in Starburst99, but the H-band spectra are full of such absorption features, making the continuum level extremely hard to determine. The Si I and CO (6-3) absorption features in the sample spectra are also very weak and do not appear in all of the galaxies. Therefore these features cannot be used in this analysis. This is unfortunate as these two features have the power to break the age-metallicity degeneracy of measurements of the stronger but more unreliable CO (2-0) band (Origlia, Moorwood, & Oliva 1993; Oliva et al. 1999).

Brackett  $\gamma$  has a clear signal in all of the spectra and the measurement of the equivalent width provides a consistent, unambiguous way to determine the age of the starburst. The Brackett  $\gamma$  equivalent width of the Starburst 99 models is sensitive to metallicity only at very low  $Z$ -values, which we do not expect nuclear populations to have. The equivalent width of Brackett  $\gamma$  has been measured from the average nuclear spectrum and is quoted along with its error in Table 4. We have chosen to use model C, the continuous star formation model with a power law of 2.35 and an upper mass cut-off of 30  $M_{\odot}$ . Selecting the lower mass cut off is more reasonable for stars forming in a high metallicity region because cooling caused by metals in pre-stellar clouds does not allow many very large stars to form. The Salpeter IMF approximated by the reference case predicts unreasonably large ages based on the equivalent width of Brackett  $\gamma$ . Figure 6 shows all three options for the IMF provided by Leitherer et al. (1999) in relation to our calculated values. The age that the model C estimates based on the strength of Brackett  $\gamma$  is shown in column three of Table 4.

The [Fe II] 1.6440  $\mu\text{m}$  emission line is not included with the Starburst99 diagnostics but the flux from this line is directly related to the supernova rate which is available as a diagnostic. This relation has recently been recalibrated by Alonso-Herrero et al. (2003) through observations of supernova remnants in the nearby galaxies M82 and NGC 253. They estimate the supernova rate as  $(\text{SNr}) = 0.8L_{[\text{FeII}]} \times 10^{-34} \text{ W}^{-1} \text{ yr}^{-1}$ . The flux from the [Fe II] line has been summed over the entire IFU and is shown in Table 4. The luminosity of this line was obtained using the distance for each galaxy listed in Table 1. Also listed in Table 4 are the supernova rates estimated by the relation above. Using the measured supernova rate and the Starburst99 age determined by Brackett  $\gamma$

we can determine the proper scaling of the normalized star formation rate and other quantities which are dependent on it, including the K-band magnitude  $M_K$ .

To determine the absolute K-band magnitude from the data cube spectra, flux was integrated in wavelength from 1.9 to 2.4  $\mu\text{m}$ . Flux was turned into a luminosity using the assumed distance listed in table 1 then  $M_K$  was found. The K-band absolute magnitude is given by Starburst99 as a function of age. The magnitude is for a star formation law producing stars at the rate of 1  $M_{\odot} \text{ yr}^{-1}$  so it must be scaled by the proper star formation rate before comparison with any measured values. The K-band magnitudes for the ages estimated by the Brackett  $\gamma$  equivalent width and scaled by this method are shown in Table 4.

#### 4.2. IC 3639

IC 3639 gives a very consistent picture of recent or ongoing nuclear star formation. The strength of Brackett  $\gamma$  and the presence of He I mean that there are still many young stars on the main sequence, but there is also a large flux from the [Fe II] line, meaning that the starburst is very vigorous. The continuous starburst model predicts a vigorous starburst producing about 5  $M_{\odot}$  per year at an age of 24 Myr. The difference between the measured K-band magnitude and the predicted starburst magnitude imply a 30% contribution to the continuum flux from the new stars.

#### 4.3. MRK 477

Markarian 477 is a very interesting galaxy because of its very strong Seyfert 2 and apparent starburst population and there are several reasons why the continuous star formation model we have applied does not work well. This galaxy has a large equivalent width of Brackett  $\gamma$  which would imply a very fairly young age. The measurement of equivalent width is dependent on the depth of the continuum which, for this galaxy, is dominated by the rising power law of the AGN and not the thermal continuum of the bright starburst. The AGN may also be a source of Brackett  $\gamma$  flux itself, contaminating the measurement further. The supernova rate at about 1 per year is high but not unreasonable, however the star formation rate that this implies is exorbitant at almost 160 solar masses per year. The final sign that the model is not correct comes from the K-band magnitude which predicts a starburst of almost the same brightness as the measured value, which cannot be correct. The AGN is contributing a large amount of additional continuum flux to the starburst. It is tempting to suggest that the massive [Fe II] flux from this galaxy might also be caused by the strong AGN at the center, which may actually be the case. Winge et al. (2000) indicate that the [Fe II] line may be produced by ionizing sources other than SNR. However it is instructive to apply an instantaneous starburst model as suggested in Heckman et al. (1997) using the same parameters used in the continuous model. Brackett  $\gamma$  is not particularly sensitive to metallicity or choice of IMF parameters for the instantaneous model and selects an age of 6 Myr. The supernova rate at this age for an instantaneous population of  $10^6 M_{\odot}$  is about 0.001 per year, which gives a scaling relation of  $10^9 M_{\odot}$  for the population of MRK 477. Finally, the scaled K-band magnitude is -23.5, a much more reasonable num-

ber for a galaxy with an enormously bright AGN. The starburst population contributes 30% of the light in the infrared. Heckman et al. (1997) estimate a 10% ultraviolet flux contribution from the starburst to the total UV flux of the nucleus. Figures 9-11 show the details of analysis with the instantaneous star formation model.

#### 4.4. NGC 2623

From the Starburst 99 continuous model predictions this object appears to be of intermediate age and still forming stars. A deep CO (2-0) absorption band and rich absorption in the H-band mean that the nucleus is full of late type stars. The [Fe II] emission is fairly small and only just rises above the continuum, but predicts a large supernova rate. The young star indicator Brackett  $\gamma$  is very strong. The Starburst99 model gives an age of 36 Myr and a k-band flux which is 10% of the observed flux. All of these factors together, and the fact that we do not observe an active nucleus in this merger means that the old, original bulge population is quite bright.

#### 4.5. NGC 3227

The nucleus of NGC 3227 contains an old stellar population which is the remnant of a starburst. This galaxy also contains a Seyfert 1 nucleus which is providing an undetermined amount of the continuum flux so the Starburst 99 age of 270 Myr should be taken as an absolute upper limit. The model predicts a 40% contribution to the light of the galaxy from the starburst, which does not seem unreasonable if the AGN is also weak from a lack of new material from supernovae.

Based on the emission spectra of the galaxies IC 3639, MRK 477, NGC 2623, and NGC 3227, all of these galaxies contain recently formed populations of new stars in their nucleus. IC 3639 has a healthy population of young stars and is well described by a continuous star forming age of 24 Myr is contributing 30% of the light to the K-band continuum. The nuclear star population in MRK 477 is better described by an instantaneous star forming model of 6 Myr which implies that it contributes 30% of the K-band flux. NGC 2623 has a supernova rate which is high but is well described by the continuous model. The starburst population is producing only 10% of the K-band flux so the old stellar population in the bulge of this galaxy is also quite important to the light output. NGC 3227 appears to have an old starburst population of 240 Myr predicted by the continuous star forming model which contributes 40% of the nuclear K-band flux. We have confirmed the presence of a composite nuclei in three of these galaxies. IC 3639 and MRK 477 each have strong Seyfert 2 nucleus in addition to their nuclear starburst. NGC 3227 has a slightly weaker Seyfert 1 nucleus whose lack of strength may be due to the decline of supernova outflows from the aging starburst. We observe no AGN activity in NGC 2623 but note that it must have a significant old nuclear population of stars. The AGN and old bulge populations of stars contribute a significant amount of continuum flux and need to be well characterized before applying stellar synthesis models to get a more accurate picture of the star formation history in these galaxies.

## 5. CONCLUSIONS

## REFERENCES

- Alonso-Herrero, A., et al., 2003, The [Fe II] 1.644 Micron Emission in M82 and NGC 253: Is it a Measure of the Supernova Rate?, *AJ*, 125, 1210.
- Barnes, J. E. & Hernquist, L., 1996, Transformations of Galaxies. II. Gasdynamics in Merging Disk Galaxies, *ApJ*, 471, 115.
- Bendo, G. J. & Joseph, R. D., 2004, Nuclear Stellar Populations in the Infrared Space Observatory Atlas of Bright Spiral Galaxies, *ApJ*, 127, 3338-3360.
- Bransford, M. A. & Appleton, P. N. et al., 1998, Radio-Luminous Southern Seyfert Galaxies. I. Radio Images and Selected Optical/Near-Infrared Spectroscopy, *ApJ*, 497, 133.
- Davies, R. I. et al., 2006, The Star-Forming Torus and Stellar Dynamical Black Hole Mass in the Seyfert 1 Nucleus of NGC 3227, *ApJ*, 646, 754.
- Ghosh, H. et al., 2007, CHANDRA Observations of Candidate "True" Seyfert 2 Nuclei, *ApJ*, 656, 105.
- Gonzalez-Delgado, R. M., Heckman, T., & Leitherer, C., 2001, The Nuclear and Circumnuclear Stellar Population in Seyfert 2 Galaxies: Implications for the Starburst-Active Galactic Nucleus Connection, *ApJ*, 546, 845.
- Gonzalez-Delgado, R. M. et al., 1998, Ultraviolet-Optical Observations of the Seyfert 2 Galaxies NGC 7130, NGC 5135, and IC 3639: Implications for the Starburst-Active Galactic Nucleus Connection, *ApJ*, 505, 174.
- Gunn, J. E., 1977, Feeding the Monster: Gas Discs in Elliptical Galaxies, in *Active Galactic Nuclei*, eds. C. Hazard & S. Mitton (Cambridge: Cambridge Univ. Press), 213.
- Heckman, T. M., et al., 1997, A Powerful Starburst in the Seyfert Galaxy Markarian 477: Implications for the Starburst-Active Galactic Nucleus Connection, *ApJ*, 482, 114.
- Kudritzki, R. P., 1998, Quantitative Spectroscopy of the Brightest Blue Stars in Galaxies, in *Stellar Astrophysics for the Local Group*, ed. A. Aparicio & A. Herrero (Cambridge: Cambridge Univ. Press), 149.
- Leitherer, C. et al., 1999, Starburst99: Synthesis Models for Galaxies with Active Star Formation, *ApJS*, 123, 3-40.
- Lipari, S. et al., 2004, Infrared Mergers and Infrared Quasi-Stellar Objects with Galactic Winds-I. NGC 2623: Nuclear Outflow in a Proto-Elliptical Candidate, *MNRAS*, 348, 369.
- Oliva, E. et al., 1999, Starbursts in Active Galaxy Nuclei: Observational Constraints from IR Stellar Absorption Lines, *A&A*, 350, 9-16.
- Origilia, L., Moorwood, A.F.M., & Oliva, E., 1993, The 1.5-1.7  $\mu$ m Spectrum of Cool Stars: Line Identifications for Spectral Classification and the Stellar Content of the Seyfert Galaxy NGC 1068, *A&A*, 280, 536.
- Ramasy-Howat, S. et al., 2004, The Commissioning of and First Results from the UIST Imager Spectrometer, *SPIE*, 5492, 1160-1171.
- Schweizer, F. & Seitzer, P., 2007, Remnant of a "Wet" Merger: NGC 34 and Its Young Massive Clusters, Young Stellar Disk, and Strong Gaseous Outflow, *AJ*, 133, 2132.
- Storchi-Bergmann, T. et al., 2001, Circumnuclear Stellar Population, Morphology, and Environment of Seyfert 2 Galaxies: An Evolutionary Scenario, *ApJ*, 559, 147.
- van der Werf, P. P. et al., 1993, Near Infrared Imaging of NGC 6240: Collision Shock and Nuclear Starburst, *ApJ*, 405, 522.
- Winge, C. et al., 2000, Extended Gas in Seyfert Galaxies: Near-Infrared Observations of 15 Active Nuclei, *MNRAS*, 316, 1.

TABLE 1  
PHYSICAL PROPERTIES OF THE GALAXIES <sup>a</sup>

Galaxy	EquJ2000(RA, Dec)	cz[km s <sup>-1</sup> ] <sup>b</sup>	Distance (Mpc)	Morphological Type	Nuclear Activity
IC 3639	12:40:52.8, -36:45:21	3275	49.6 ± 3.5	SB(rs)bc	Sy 2
MRK 477	14:40:38.1, +53:30:16	11310	158.1 ± 11.1	Compact	Sy 2
NGC 2623	08:38:24.1, +25:45:17	5549	75.9 ± 5.3	Pec	Sy 2
NGC 3227	10:23:30.6, +19:51:54	1157	18.3 ± 1.3	SAB(s) pec	Sy 1.5

<sup>a</sup> Coordinates, Distance, Morphological Type, and Nuclear Activity come from NED

<sup>b</sup> Distance used is corrected for Virgo+GA+Shapley and assumes  $H=73 \pm 5 \text{ km s}^{-1} \text{ Mpc}^{-1}$

TABLE 2  
SPECTRAL DIAGNOSTICS

Diagnostic	Wavelength( $\mu\text{m}$ ) <sup>a</sup>	Indicates
Si I	1.5890	Red giant stars
CO 6-3 band head	1.6189	Red giant stars
[Fe II]	1.6440	Supernova remnants
Paschen $\alpha$	1.8756	O & B main sequence stars, AGN
H <sub>2</sub> 1-0 S(3)	1.9576	Shocked neutral medium
[Si VI]	1.9634	AGN
H <sub>2</sub> 1-0 S(2)	2.0338	Shocked neutral medium
He I	2.0587	Windy O & B main sequence stars
H <sub>2</sub> 1-0 S(1)	2.1218	Shocked neutral medium
Brackett $\gamma$	2.1661	O & B main sequence stars, AGN
CO 2-0 band head	2.2935	Red giant stars

<sup>a</sup> Wavelength data is from Allen's Astrophysical Quantities

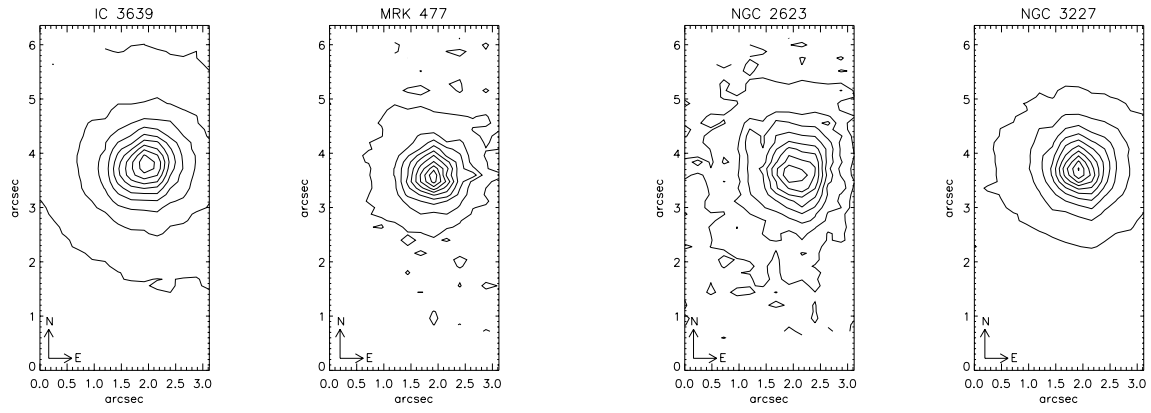


FIG. 1.— Contour maps of the intensity summed from 1.4-2.4  $\mu\text{m}$  for the four galaxies in the sample, from left to right: IC 3639, MRK 477, NGC 2623, and NGC 3227. Note that North is up and East is right.

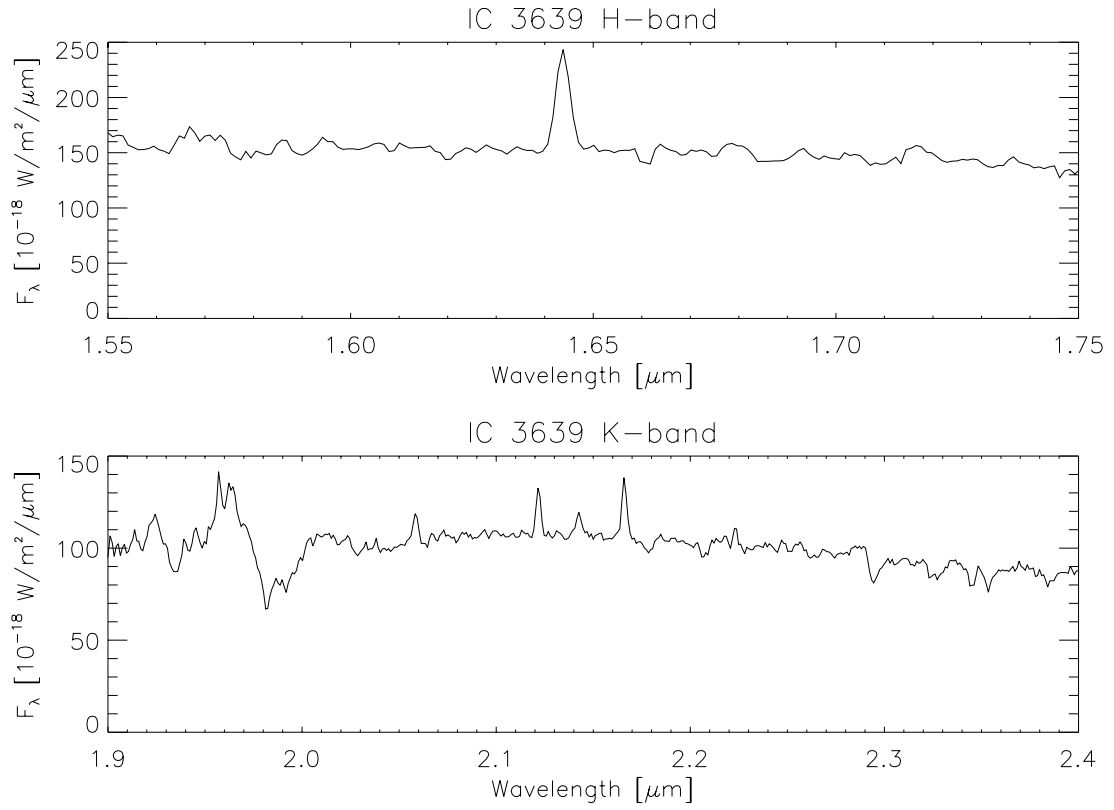


FIG. 2.— The averaged H-band spectrum (top) and K-band spectrum (bottom) of nuclear region of IC 3639.

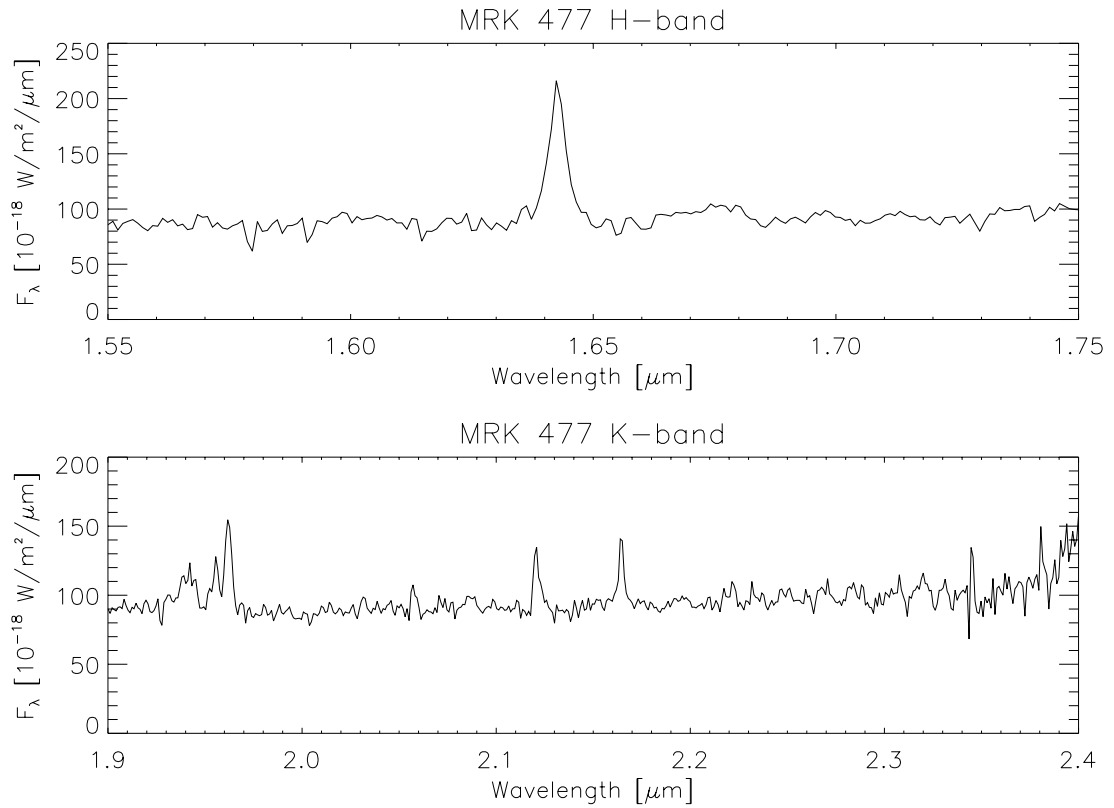


FIG. 3.— The averaged H-band spectrum (top) and K-band spectrum (bottom) of nuclear region of MRK 477.

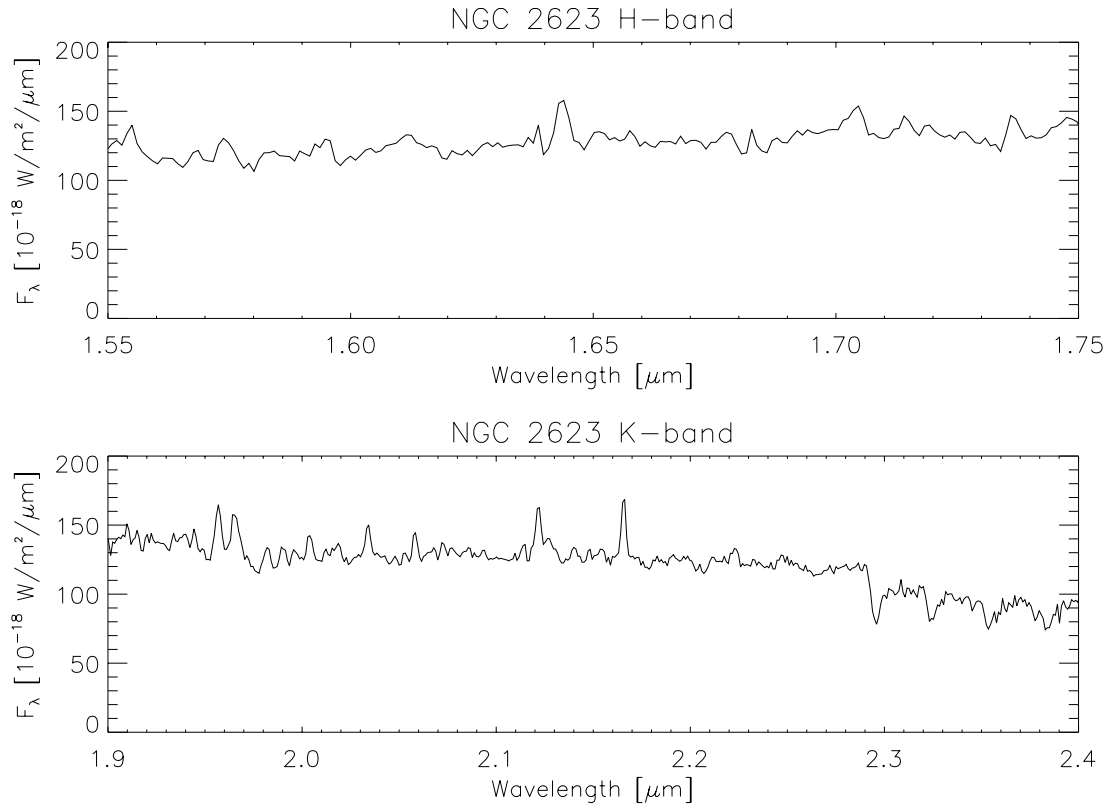


FIG. 4.— The averaged H-band spectrum (top) and K-band spectrum (bottom) of nuclear region of NGC 2623.

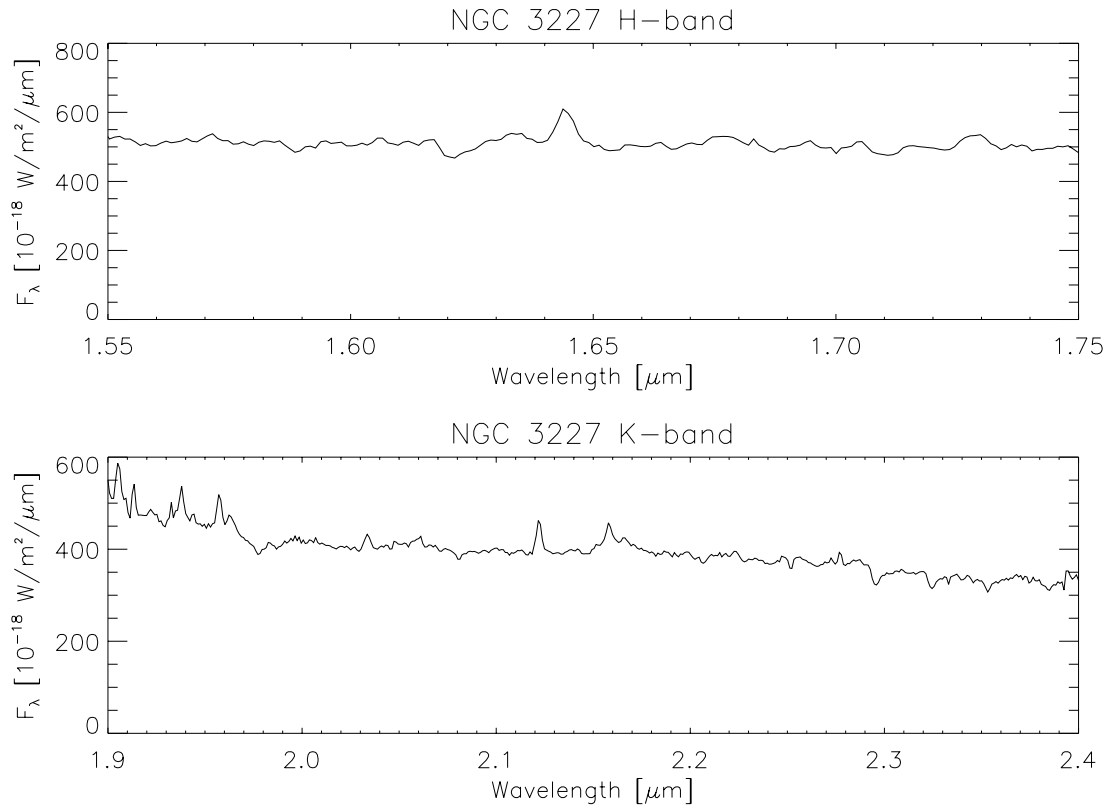


FIG. 5.— The averaged H-band spectrum (top) and K-band spectrum (bottom) of nuclear region of NGC 3227.



TABLE 4  
STARBURST 99 DIAGNOSTICS

Galaxy	$\log W(\text{Br}\gamma[\text{\AA}])$	Age [Myr] <sup>a</sup>	$F_{[\text{FeII}]}$ <sup>b</sup>	SNR [ $\text{yr}^{-1}$ ]	SFR [ $M_{\odot} \text{yr}^{-1}$ ]	$M_K$ measured	$M_K$ predicted
IC 3639	$1.07 \pm 0.02$	$24 \pm 2$	$1.89 \pm 0.5$	$0.045 \pm 0.004$	$3.45 \pm 0.40$	$-22.7 \pm 0.2$	$-21.2 \pm 0.1$
MRK 477	$1.20 \pm 0.05$	$14 \pm 3$	$4.29 \pm 0.2$	$1.03 \pm 0.08$	$159 \pm 5.0$	$-24.8 \pm 0.2$	$-25.0 \pm 0.1$
NGC 2623	$0.99 \pm 0.02$	$36 \pm 4$	$1.45 \pm 0.1$	$0.080 \pm 0.03$	$4.36 \pm 1.5$	$-23.9 \pm 0.2$	$-21.7 \pm 0.4$
NGC 3227	$0.68 \pm 0.05$	$270 \pm 10$	$4.40 \pm 0.1$	$0.014 \pm 0.002$	$0.75 \pm 0.11$	$-21.6 \pm 0.2$	$-20.5 \pm 0.2$

<sup>a</sup> The age is that predicted by the Starburst99 model.

<sup>b</sup> Flux units are [ $10^{-17} \text{ W m}^{-2}$ ].

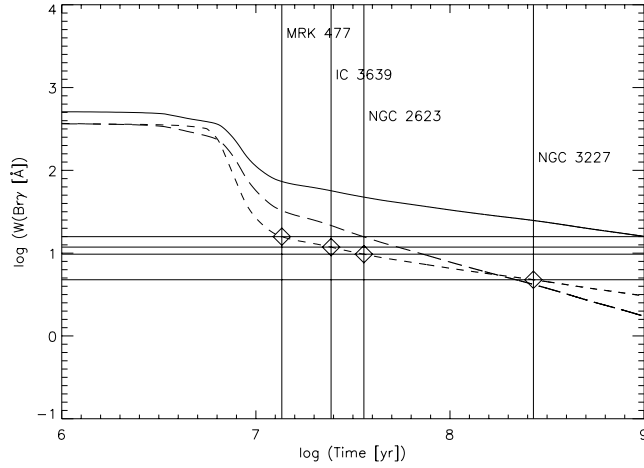


FIG. 6.— The  $\log(W(\text{Br}\gamma))$  values for our galaxies (horizontal solid lines) compared to the predicted  $\log(W(\text{Br}\gamma))$  vs. time using the  $Z=0.020$  continuous star formation models from Leitherer et al. (1999). Star formation law: model A, solid line; model B, long dashed line; model C, short dashed line. Ages predicted by model C are indicated by the vertical solid lines. Refer to Table 4 for relevant quantities and their errors.

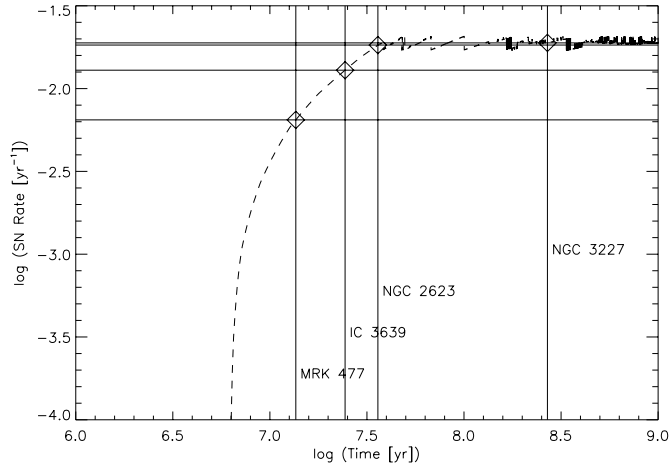


FIG. 7.— The  $\log(\text{SNR})$  vs. time predicted by model C, normalized to  $1 M_{\odot} \text{ yr}^{-1}$  of star formation (short dashed line). Ages predicted above (vertical solid lines) for each of the galaxies imply a  $\log(\text{SNR})$  from the model (horizontal solid lines) which gives the proper scaling for quantities dependent on the number of stars. Refer to Table 4 for relevant quantities and their errors.

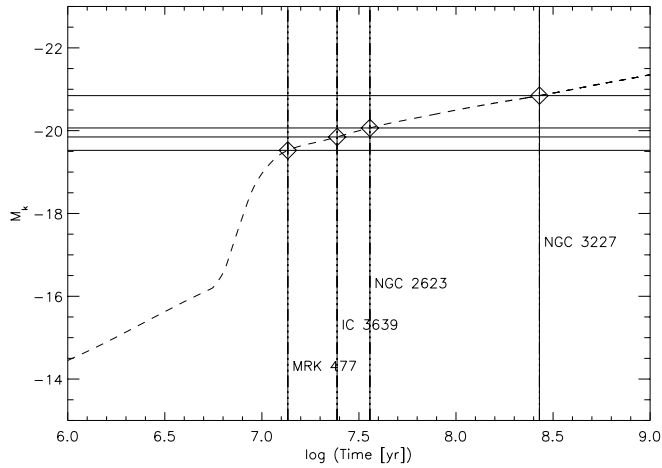


FIG. 8.— The K-band magnitude vs. time for model C, normalized to  $1 M_{\odot} \text{ yr}^{-1}$  of star formation (short dashed line). Ages predicted above (vertical solid lines) for each of the galaxies imply an  $M_K$  from the model (horizontal solid lines) which can be scaled and compared to the measured  $M_K$ . Refer to Table 4 for relevant quantities and their errors.

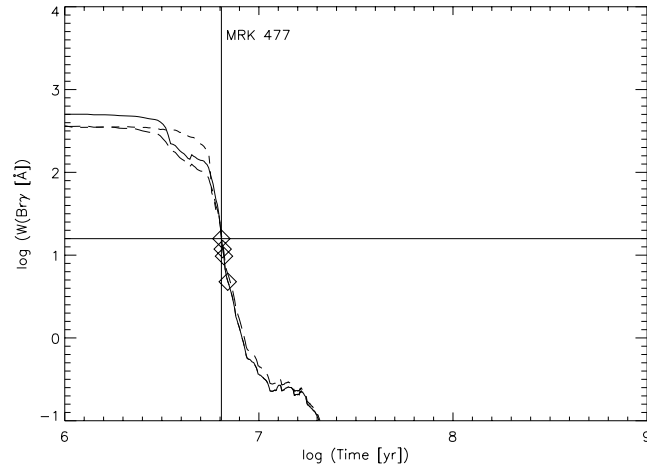


FIG. 9.— The  $\log(W(\text{Br}\gamma))$  values for MRK 477 (horizontal solid line) compared to the predicted  $\log(W(\text{Br}\gamma))$  vs. time using the  $Z=0.020$  instantaneous star formation models from Leitherer et al. (1999). Star formation law: model A, solid line; model B, long dashed line; model C, short dashed line. The age of MRK 477 predicted by model C is indicated by the vertical solid line. Diamonds indicate the measured values and the values predicted by the model for all the galaxies.

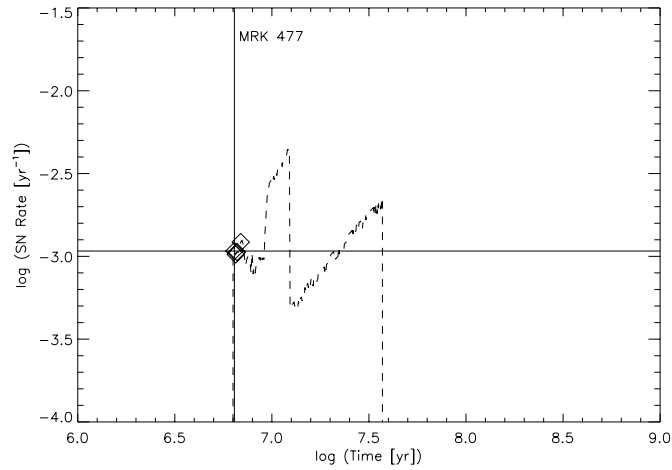


FIG. 10.— The  $\log(\text{SNR})$  vs. time predicted by model C, normalized to  $10^6 M_{\odot}$  of instantaneous star formation (short dashed line). The age of MRK 477 predicted above (vertical solid line) implies a  $\log(\text{SNR})$  from the model (horizontal solid line) which gives the proper scaling for  $M_K$ .

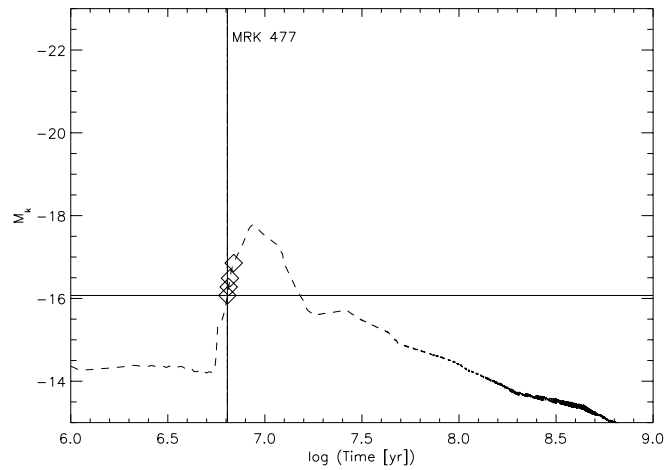


FIG. 11.— The K-band magnitude vs. time for model C, normalized to  $10^6 M_{\odot}$  of instantaneous star formation (short dashed line). The age of MRK 477 predicted above (vertical solid line) implies an  $M_K$  from the model (horizontal solid line) which can be scaled and compared to the measured  $M_K$ .